Inorg. Chem. **2003**, *42*, 3423–3430

Examination of Novel Zinc-Binding Groups for Use in Matrix Metalloproteinase Inhibitors

David T. Puerta and Seth M. Cohen*

Department of Chemistry and Biochemistry, University of California, San Diego, La Jolla, California 92093-0358

Received September 12, 2002

The tetrahedral zinc complex [($Tp^{Ph,Me}$)ZnOH] ($Tp^{Ph,Me}$ = hydrotris(3,5-phenylmethylpyrazolyl)borate) was combined with 1-hydroxy-2(1*H*)-pyridinone, 3-hydroxy-2(1*H*)-pyridinone, 3-hydroxy-1-methyl-2(1*H*)-pyridinone, 3-hydroxy-1,2-dimethyl-4(1*H*)-pyridinone, 1-hydroxy-2(1*H*)-pyridinethione, and 3-hydroxy-2-methyl-4-pyrone to generate the complexes [($Tp^{Ph,Me}$)Zn(ZBG)] (ZBG = zinc-binding group). These complexes were synthesized to explore the coordination geometry of potential novel zinc-binding groups for use in matrix metalloproteinase (MMP) inhibitors. The solid-state structures of all six metal complexes were determined by X-ray crystallography. These structures combined with IR and ^{1}H NMR data demonstrate that these ZBGs bind in a strong, bidentate fashion to the zinc(II) ion. Modeling studies indicate that these ZBGs can easily fit into the MMP active site. In an effort to develop more effective inhibitors of MMPs, this work has revealed molecular-level interactions for six potential new ZBGs.

Introduction

Matrix metalloproteinases (MMPs) are zinc(II)-containing hydrolytic enzymes that are involved in the breakdown of the extracellular matrix. The activity of these enzymes is often associated with illnesses such as cancer, arthritis, and inflammatory disease.[1−3] The correlation between MMP activity and these debilitating diseases has made these hydrolytic enzymes targets of drug-based inhibition. However, despite the evaluation of thousands of compounds, no matrix metalloproteinase inhibitors (MPIs) have completed phase III clinical trials.[4]

Many factors must be considered in designing an effective and selective drug. In the case of MPIs, the drug typically consists of two parts, a peptidomimetic backbone and a zinc-binding group (ZBG). The backbone serves as a substrate analogue, allowing the inhibitor to fit in the active-site cleft of the enzyme. The ZBG is crucial for binding to the catalytic zinc(II) ion, thereby rendering the MMP inactive. The vast majority of MPI investigations have focused on improving the backbone interactions of MPIs while opting to use a common ZBG, namely a hydroxamic acid moiety, that has been in regular use for more than 20 years.[1] Although extensive efforts have been made to improve MPIs by manipulating the substrate-like backbone of the drug, significantly fewer efforts have concentrated on improving the ZBG.[3] The exploration and discovery of more potent and selective ZBGs is required to take MPIs toward a more productive second generation of development.

Previous work has shown that tris(pyrazolyl)borate complexes of zinc provide an accurate model for the tris(histidine) active site of several metalloproteins including MMPs.[5−8] In addition, some of these model compounds have shown that acetohydroxamic acid forms a complex (Scheme 1) that is structurally identical to the coordination environment of hydroxamate-based drugs bound to the catalytic zinc(II) ion in MMPs.[9,10] Using this same model, we evaluated the interaction of ZBGs from identified inhibitors where the mode of binding was unknown.[11−13] This study proved to

* To whom correspondence should be addressed. Telephone: (858) 822-5596. Fax: (858) 822-5598. E-mail: scohen@ucsd.edu.

(1) Whittaker, M.; Floyd, C. D.; Brown, P.; Gearing, A. J. H. *Chem. Rev.* **1999**, *99*, 2735−2776 and references therein.
(2) Brinckerhoff, C. E.; Matrisian, L. M. *Nat. Rev. Mol. Cell Biol.* **2002**, *3*, 207−214.
(3) Overall, C. M.; López-Otín, C. *Nat. Rev. Cancer* **2002**, *2*, 657−672.
(4) Coussens, L. M.; Fingleton, B.; Matrisian, L. M. *Science* **2002**, *295*, 2387−2392.
(5) Puerta, D. T.; Cohen, S. M. *Inorg. Chim. Acta* **2002**, *337*, 459−462.
(6) Trofimenko, S. *Chem. Rev.* **1993**, *93*, 943−980.
(7) Parkin, G. *Chem. Commun.* **2000**, 1971−1985.
(8) Vahrenkamp, H. *Acc. Chem. Res.* **1999**, *32*, 589−596.
(9) Ruf, M.; Weis, K.; Brasack, I.; Vahrenkamp, H. *Inorg. Chim. Acta* **1996**, *250*, 271−281.
(10) Puerta, D. T.; Cohen, S. M. *Inorg. Chem.* **2002**, *41*, 5075−5082.
(11) Levin, J. I.; DiJoseph, J. F.; Killar, L. M.; Sharr, M. A.; Skotnicki, J. S.; Patel, D. V.; Xiao, X.-Y.; Shi, L.; Navre, M.; Campbell, D. A. *Bioorg. Med. Chem. Lett.* **1998**, *8*, 1163−1168.

10.1021/ic026029g CCC: $25.00
Published on Web 05/02/2003

Scheme 1. Synthesis of [(Tp^{Ph,Me})Zn(ZBG)] Model Complexes (ZBG = Zinc-Binding Group)

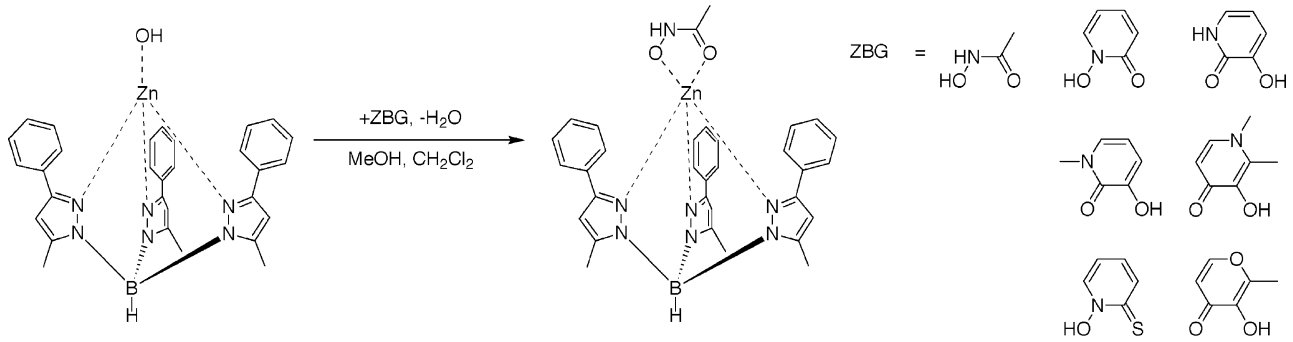

be very informative, because a direct correlation between the inhibitory activity and mode of binding was found.[10] These observations further validated the use of model complexes as an effective strategy for determining, at a molecular level, the interactions between inhibitors and MMPs.

In a continuing effort to elucidate drug−metalloprotein interactions by using bioinorganic model compounds, this report describes the binding of several new ZBGs that show promise for incorporation into second-generation MMP inhibitors. The complexes presented in this paper demonstrate that tris(pyrazolyl)borate complexes of zinc(II) can be used as an initial screen for ZBGs by providing structural and qualitative binding information without the need for sophisticated drug synthesis or protein structure determination. Six ligands were selected to demonstrate the wide range of compounds that might serve as effective ZBGs. These ligands share several features in common with the regularly utilized hydroxamate ZBG because these compounds are monoanionic ligands that were anticipated to bind the zinc ion in a chelating bidentate fashion. The compounds studied were also selected because of their potential biocompatibility based on their presently known uses in biological systems (vide infra). The data herein demonstrate that the ZBGs, 1-hydroxy-2(1*H*)-pyridinone, 3-hydroxy-2(1*H*)-pyridinone, 3-hydroxy-1-methyl-2(1*H*)-pyridinone, 3-hydroxy-1,2-dimethyl-4(1*H*)-pyridinone, 1-hydroxy-2(1*H*)-pyridinethione, and 3-hydroxy-2-methyl-4-pyrone each displace the hydroxide ligand in [(Tp^{Ph,Me})ZnOH] and coordinate the zinc(II) ion in a bidentate fashion. The metal−ligand bond lengths are compared to those found in the corresponding acetohydroxamate complex.[10] The model-based approach described here is expected to provide an unexplored and effective route toward second-generation MPI design.

Experimental Section

General. Unless otherwise noted, starting materials were obtained from commercial suppliers (Aldrich) and used without further purification. [(Tp^{Ph,Me})ZnOH][5] and 3-hydroxy-1-methyl-2(1*H*)-pyridinone[14−16] were synthesized as previously described. Elemental analysis was performed at the University of California, Berkeley Analytical Facility. ^{1}H/^{13}C NMR spectra were recorded on a Varian FT-NMR spectrometer running at 300 or 400 MHz at the Department of Chemistry and Biochemistry, University of California, San Diego. Infrared spectra were collected on a Nicolet AVATAR 320 FT-IR instrument at the Department of Chemistry and Biochemistry, University of California, San Diego. *Caution! Perchlorate salts of metal complexes with organic ligands are potentially explosive. Only small amounts of these materials should be prepared, and they should be handled with great care.*

[(Tp^{Ph,Me})Zn(1-hydroxy-2(1*H*)-pyridinone)]. In a 100-mL round-bottom flask, [(Tp^{Ph,Me})ZnOH] (145 mg, 0.26 mmol) was added to 10 mL of CH_2Cl_2. To this solution was added 1.0 equiv of 1-hydroxy-2(1*H*)-pyridinone (29 mg, 0.26 mmol) dissolved in 15 mL of MeOH. The mixture was stirred at room temperature overnight under a nitrogen atmosphere. After stirring, the turbid solution was evaporated to dryness on a rotary evaporator to give a white solid. The solid was dissolved in a minimum amount of benzene (~15 mL) and filtered to remove any insoluble material, and the filtrate was recrystallized by diffusion of the solution with pentane. Yield: 94%. ^{1}H NMR ($CDCl_3$, 400 MHz, 25 °C): δ 2.51 (s, 9H, pyrazole-CH_3), 5.78 (d, J = 8.0 Hz, 1H, pyridinone-H), 6.10 (t, J = 6.4 Hz, 1H, pyridinone-H), 6.17 (s, 3H, pyrazole-H), 6.84 (t, J = 7.0 Hz, 1H, pyridinone-H), 7.10 (m, 9H, phenyl-H), 7.58 (d, J = 6.8 Hz, 6H, phenyl-H), 7.67 (d, J = 8.0 Hz, 1H, pyridinone-H). ^{13}C NMR ($CDCl_3$, 100 MHz, 25 °C): δ 13.0, 104.4, 106.8, 113.8, 127.2, 127.3, 127.6, 131.4, 132.8, 134.0, 144.7, 152.6, 159.9 (C=O). IR (film from $CHCl_3$): ν 1370, 1537, 1625, 2546 (B−H) cm^{-1}. Anal. Calcd for $C_{35}H_{32}BN_7O_2Zn$: C, 63.80; H, 4.90; N, 14.88. Found C, 63.69; H, 4.91; N, 15.14.

[(Tp^{Ph,Me})Zn(3-hydroxy-2(1*H*)-pyridinone)]. The same procedure was used as in the synthesis of [(Tp^{Ph,Me})Zn(1-hydroxy-2(1*H*)-pyridinone)]. Yield: 76%. ^{1}H NMR ($CDCl_3$, 400 MHz, 25 °C): δ 2.51 (s, 9H, CH_3, pyrazole-CH_3), 6.00 (m, 1H, pyridinone-H), 6.08 (t, J = 7.4 Hz, 1H, pyridinone-H), 6.18 (s, 3H, pyrazole-H), 6.39 (d, J = 6.8 Hz, 1H, pyridinone-H), 7.10 (t, J = 6.0 Hz, 9H, phenyl-H), 7.61 (m, 6H, phenyl-H). ^{13}C NMR ($CDCl_3$, 100 MHz, 25 °C): δ 13.0, 104.2, 110.2, 113.6, 113.8, 127.1, 127.4, 127.5, 132.4, 144.7, 152.5, 155.8, 162.6 (C=O). IR (film from $CHCl_3$): ν 1305, 1546, 1619, 2547 (B−H) cm^{-1}. Anal. Calcd for $C_{35}H_{32}BN_7O_2Zn$: C, 63.80; H, 4.90; N, 14.88. Found C, 63.61; H, 5.03; N, 14.91.

[(Tp^{Ph,Me})Zn(3-hydroxy-1-methyl-2(1*H*)-pyridinone)]. The same procedure was used as in the synthesis of [(Tp^{Ph,Me})Zn(1-hydroxy-2(1*H*)-pyridinone)]. Yield: 80%. ^{1}H NMR ($CDCl_3$, 400 MHz, 25 °C): δ 2.55 (s, 9H, pyrazole-CH_3), 3.50 (s, 3H, pyridinone-CH_3), 6.01 (t, J = 6.8 Hz, 1H, pyridinone-H), 6.24 (s, 3H, pyrazole-

(12) Campbell, D. A.; Xiao, X.-Y.; Harris, D.; Ida, S.; Mortezaei, R.; Ngu, K.; Shi, L.; Tien, D.; Wang, Y.; Navre, M.; Patel, D. V.; Sharr, M. A.; DiJoseph, J. F.; Killar, L. M.; Leone, C. L.; Levin, J. I.; Skotnicki, J. S. *Bioorg. Med. Chem. Lett.* **1998**, *8*, 1157−1162.
(13) Baxter, A. D.; Bird, J.; Bhogal, R.; Massil, T.; Minton, K. J.; Montana, J.; Owen, D. A. *Bioorg. Med. Chem. Lett.* **1997**, *7*, 897−902.
(14) Xu, J.; Franklin, S. J.; Whisenhunt, D. W., Jr.; Raymond, K. N. *J. Am. Chem. Soc.* **1995**, *117*, 7245−7246.
(15) Raymond, K. N.; Xu, J. U.S. Patent 5,892,029, 1999.
(16) Raymond, K. N.; Xu, J. U.S. Patent 5,624,901, 1997.

Table 1. Crystal Data for [(Tp^{Ph,Me})Zn(1-hydroxy-2(1*H*)-pyridinone)], [(Tp^{Ph,Me})Zn(3-hydroxy-2(1*H*)-pyridinone)], and [(Tp^{Ph,Me})Zn(3-hydroxy-1-methyl-2(1*H*)-pyridinone)]

	[(Tp^{Ph,Me})Zn (1-hydroxy-2(1*H*)-pyridinone)]	[(Tp^{Ph,Me})Zn (3-hydroxy-2(1*H*)-pyridinone)]	[(Tp^{Ph,Me})Zn (3-hydroxy-1-methyl-2(1*H*)-pyridinone)]
empirical formula	$C_{35}H_{32}BN_7O_2Zn$	$C_{41}H_{38}BN_7O_2Zn$	$C_{42}H_{41}BN_7O_2Zn$
cryst syst	monoclinic	triclinic	monoclinic
space group	$P2_1/c$	$P-1$	$P2_1/c$
unit cell dimensions	$a = 9.7863(15)$ Å $\alpha = 90°$ $b = 23.269(4)$ Å $\beta = 98.122(3)°$ $c = 13.607(2)$ Å $\gamma = 90°$	$a = 11.0865(10)$ Å $\alpha = 111.300(10)°$ $b = 12.229(11)$ Å $\beta = 96.615(2)°$ $c = 15.469(14)$ Å $\gamma = 102.364(2)°$	$a = 19.959(2)$ Å $\alpha = 90°$ $b = 16.652(19)$ Å $\beta = 92.197(2)°$ $c = 10.988(12)$ Å $\gamma = 90°$
vol, Z	3067.5(8) Å^3, 4	1865.3(3) Å^3, 2	3649.4(7) Å^3, 4
cryst size	$0.20 \times 0.07 \times 0.07$ mm^3	$0.35 \times 0.20 \times 0.06$ mm^3	$0.26 \times 0.15 \times 0.06$ mm^3
T (K)	100(1)	100(1)	100(1)
reflns collected	26 190	10 782	31 063
independent reflns	7029 [R(int) = 0.0620]	7642 [R(int) = 0.0150]	8344 [R(int) = 0.0540]
data/restraints/params	7029/0/422	7642/0/516	8344/0/486
GOF on F^2	0.882	1.067	0.941
final R indices $I > 2\sigma(I)$	$R1 = 0.0435$ w$R2 = 0.0797$	$R1 = 0.0589$ w$R2 = 0.1714$	$R1 = 0.0374$ w$R2 = 0.0866$
R indices (all data)	$R1 = 0.0781$ w$R2 = 0.0864$	$R1 = 0.0676$ w$R2 = 0.1802$	$R1 = 0.0481$ w$R2 = 0.0897$
largest peak/hole difference	0.836/−0.567 e Å^{-3}	1.464/−0.458 e Å^{-3}	0.767/−0.484 e Å^{-3}

H), 6.68 (t, $J = 5.6$ Hz, 1H pyridinone-H), 7.22 (m, 9H, phenyl-H), 7.45 (d, $J = 5.6$ Hz, 1H pyridinone-H), 7.56 (d, $J = 6.8$ Hz, 6H, phenyl-H). ^{13}C NMR ($CDCl_3$, 100 MHz, 25 °C): δ 13.0, 37.7, 104.0, 105.3, 128.1, 128.2, 128.6, 128.9, 130.6, 135.8, 145.8, 153.9. IR (film from $CHCl_3$): ν 1301, 1371, 1573, 2544 (B−H) cm^{-1}. Anal. Calcd for $C_{36}H_{34}N_7O_2BZn \cdot C_6H_6 \cdot H_2O$: C, 65.60; H, 5.50; N, 12.75. Found C, 65.65; H, 5.41; N, 12.84.

[(Tp^{Ph,Me})Zn(3-hydroxy-1,2-dimethyl-4(1*H*)-pyridinone)]. The same procedure was used as in the synthesis of [(Tp^{Ph,Me})Zn(1-hydroxy-2(1*H*)-pyridinone)]. Yield: 22%. ^{1}H NMR ($CDCl_3$, 400 MHz, 25 °C): δ 2.00 (s, 3H, pyridinone-CH_3), 2.51 (s, 9H, pyrazole-CH_3), 3.57 (s, 3H, pyridinone-CH_3), 5.47 (d, $J = 6.4$ Hz, 1H, pyridinone-H), 6.16 (s, 3H, pyrazole-H), 6.66 (d, $J = 6.0$ Hz, 1H, pyridinone-H), 7.04 (m, 9H, phenyl-H), 7.61 (d, $J = 5.6$ Hz, 6H, phenyl-H). ^{13}C NMR ($CDCl_3$, 100 MHz, 25 °C): δ 12.4, 13.0, 42.4, 104.4, 107.4, 126.8, 127.3, 127.6, 128.2, 132.9, 144.6, 152.5. IR (film from $CHCl_3$): ν 1367, 1553, 1594, 2547 (B−H) cm^{-1}. Anal. Calcd for $C_{37}H_{36}BN_7O_2Zn \cdot H_2O$: C, 63.04; H, 5.43; N, 13.91. Found C, 62.89; H, 5.39; N, 13.66.

[(Tp^{Ph,Me})Zn(1-hydroxy-2(1*H*)-pyridinethione)]. The same procedure was used as in the synthesis of [(Tp^{Ph,Me})Zn(1-hydroxy-2(1*H*)-pyridinone)]. Yield: 70%. ^{1}H NMR (d^6-benzene, 400 MHz, 25 °C): δ 2.26 (s, 9H, pyrazole-CH_3), 5.50 (t, $J = 7.0$ Hz, 1H, pyridinethione-H), 6.01 (s, 3H, pyrazole-H), 6.03 (t, $J = 4.8$ Hz, 1H, pyridinethione-H), 6.67 (d, $J = 8.0$ Hz, 1H, pyridinethione-H), 6.90 (t, $J = 6.2$ Hz, 3H, phenyl-H), 7.01 (t, $J = 6.8$ Hz, 6H, phenyl-H), 7.18 (m, 1H, pyridinethione-H), 7.81 (d, $J = 8.0$ Hz, 6H, phenyl-H). ^{13}C NMR ($CDCl_3$, 100 MHz, 25 °C): δ 13.0, 104.9, 116.0, 125.6, 127.1, 127.4, 128.0, 128.8, 132.9, 135.2, 144.4, 152.9. IR (film from $CHCl_3$): ν 1456, 1546, 1596, 2551 (B−H) cm^{-1}. Anal. Calcd for $C_{35}H_{32}N_7OSBZn$: C, 62.28; H, 4.78; N, 14.53. Found C, 62.17; H, 4.89; N, 14.79.

[(Tp^{Ph,Me})Zn(3-hydroxy-2-methyl-4-pyrone)]. The same procedure was used as in the synthesis of [(Tp^{Ph,Me})Zn(1-hydroxy-2(1*H*)-pyridinone)]. Yield: 61%. ^{1}H NMR ($CDCl_3$, 400 MHz, 25 °C): δ 2.23 (s, 3H, pyrone-CH_3), 2.51 (s, 9H, pyrazole-CH_3), 5.29 (d, $J = 5.2$ Hz, 1H, pyrone-H), 6.17 (s, 3H, pyrazole-H), 7.10 (m, 9H, phenyl-H), 7.18 (d, 1H, $J = 5.2$ Hz, pyrone-H), 7.59 (d, $J = 4.0$ Hz, 6H, phenyl-H). ^{13}C NMR ($CDCl_3$, 100 MHz, 25 °C): δ 13.0, 14.7, 104.3, 109.2, 127.0, 127.4, 127.5, 128.2, 132.7, 144.7, 150.4, 152.5. IR (film from $CHCl_3$): ν 1282, 1455, 1597, 2544 (B−H) cm^{-1}. Anal. Calcd for $C_{36}H_{33}N_6O_3BZn$: C, 64.16; H, 4.94; N, 12.47. Found C, 64.74; H, 5.03; N, 12.23.

X-ray Crystallographic Analysis. Data were collected on a Bruker AXS area detector diffractometer. Crystals were mounted on quartz capillaries by using Paratone oil and were cooled in a nitrogen stream (Kryo-flex controlled) on the diffractometer (−173 °C). Peak integrations were performed with the Siemens SAINT software package. Absorption corrections were applied using the program SADABS. Space group determinations were performed by the program XPREP. The structures were solved by direct or Patterson methods and refined with the SHELXTL software package.[17] Unless noted otherwise, all hydrogen atoms were fixed at calculated positions with isotropic thermal parameters; all non-hydrogen atoms were refined anisotropically.

[(Tp^{Ph,Me})Zn(1-hydroxy-2(1*H*)-pyridinone)]. Colorless blocks were grown out of a solution of the complex in benzene diffused with pentane (Table 1). The hydrogen atom on the boron was found in the difference map, and the position was refined.

[(Tp^{Ph,Me})Zn(3-hydroxy-2(1*H*)-pyridinone)]. Colorless blocks were grown within a few minutes from a solution of the complex in benzene diluted with pentane (Table 1). The hydrogen atom on the boron was found in the difference map, and its position was refined. The complex cocrystallized with one molecule of benzene that was refined to half occupancy in the asymmetric unit. The complex also contained a disordered phenyl ring on one of the pyrazole arms that was refined in two orientations (partial occupancy 55:45 split). There was no disorder observed in the coordination environment. No hydrogen atoms were calculated or refined for the disordered phenyl ring.

[(Tp^{Ph,Me})Zn(3-hydroxy-1-methyl-2(1*H*)-pyridinone)]. Colorless blocks were grown out of a solution of the complex in benzene diffused with pentane (Table 1). The hydrogen atom on the boron was found in the difference map, and the position was refined. The complex cocrystallized with one disordered molecule of benzene in the asymmetric unit. No hydrogen atoms were calculated or refined for the disordered benzene solvent molecule.

(17) Sheldrick, G. M. *SHELXTL vers. 5.1 Software Reference Manual*; Bruker AXS: Madison, WI, 1997.

Table 2. Crystal Data for [(Tp^{Ph,Me})Zn(3-hydroxy-1,2-dimethyl-4(1*H*)-pyridinone)], [(Tp^{Ph,Me})Zn(1-hydroxy-2(1*H*)-pyridinethione)], and [(Tp^{Ph,Me})Zn(3-hydroxy-2-methyl-4-pyrone)

	[(Tp^{Ph,Me})Zn (3-hydroxy-1,2-dimethyl-4(1*H*)-pyridinone)]	[(Tp^{Ph,Me})Zn (1-hydroxy-2(1*H*)-pyridinethione)]	[(Tp^{Ph,Me})Zn (3-hydroxy-2-methyl-4-pyrone)]
empirical formula	$C_{37}H_{36}BN_7O_2Zn$	$C_{140}H_{128}B_4N_{28}O_4S_4Zn_4$	$C_{36}H_{33}BN_6O_3Zn$
cryst syst	monoclinic	monoclinic	triclinic
space group	$P2_1/n$	$C2/c$	$P-1$
unit cell dimensions	$a = 12.215(14)$ Å $\alpha = 90°$ $b = 11.0738(13)$ Å $\beta = 100.944(2)°$ $c = 24.646(3)$ Å $\gamma = 90°$	$a = 35.847(3)$ Å $\alpha = 90°$ $b = 20.813(15)$ Å $\beta = 100.251(10)°$ $c = 34.388(3)$ Å $\gamma = 90°$	$a = 10.0442(8)$ Å $\alpha = 93.609(10)°$ $b = 10.376(8)$ Å $\beta = 101.606(10)°$ $c = 17.237(14)$ Å $\gamma = 93.206(10)°$
vol, Z	3273.0(7) Å^3, 4	25246(3) Å^3, 32	1751.9(2) Å^3, 2
cryst size	$0.17 \times 0.10 \times 0.02$ mm^3	$0.34 \times 0.13 \times 0.05$ mm^3	$0.35 \times 0.19 \times 0.05$ mm^3
T (K)	100(1)	100(1)	100(1)
reflns collected	27 739	108 046	14 755
independent reflns	7497 [R(int) = 0.0487]	28 818 [R(int) = 0.0484]	7606 [R(int) = 0.0192]
data/restraints/params	7497/0/422	28 818/0/1685	7606/0/459
GOF on F^2	1.008	0.990	1.047
final R indices $I > 2\sigma(I)$	$R1 = 0.0410$ w$R2 = 0.0841$	$R1 = 0.0416$ w$R2 = 0.0942$	$R1 = 0.0291$ w$R2 = 0.0792$
R indices (all data)	$R1 = 0.0617$ w$R2 = 0.0914$	$R1 = 0.0823$ w$R2 = 0.1104$	$R1 = 0.0309$ w$R2 = 0.0805$
largest peak/hole difference	0.405/−0.431 e Å^{-3}	0.645/−0.288 e Å^{-3}	0.418/−0.397 e Å^{-3}

[(Tp^{Ph,Me})Zn(3-hydroxy-1,2-dimethyl-4(1*H*)-pyridinone)]. Colorless blocks were grown out of a solution of the complex in benzene diffused with pentane (Table 2). The hydrogen atom on the boron was found in the difference map, and the position was refined.

[(Tp^{Ph,Me})Zn(1-hydroxy-2(1*H*)-pyridinethione)]. Colorless blocks were grown out of a solution of the complex in benzene diffused with pentane (Table 2). The hydrogen atoms on the boron atoms were found in the difference map, and their positions were refined. The asymmetric unit contains four molecules of the complex.

[(Tp^{Ph,Me})Zn(3-hydroxy-2-methyl-4-pyrone)]. Colorless blocks were grown out of a solution of the complex in benzene diffused with pentane (Table 2). The hydrogen atom on the boron was found in the difference map, and the position was refined. The complex cocrystallized with one-half molecule of benzene in the asymmetric unit.

Computer Modeling Analysis. Computer analysis was performed on PC workstations running a Linux (Red Hat) operating system. Superpositions were performed on the structure of human stromelysin-1 (MMP-3) by using coordinates from the Protein Data Bank (entry 1CQR, Chain A).[18,19] The coordinating pyrazole nitrogen atoms were directly superimposed onto the Nϵ2 atoms of the coordinating histidine residues in the protein. The superpostions were executed using a custom-written script[20] that overlaid the small-molecule X-ray coordinates onto the protein structure by using a least-squares fitting of the corresponding nitrogen atoms. Three different orientations were constructed for each analysis (vide infra). The resulting structures were then examined by using Rasmol (v. 2.7.2.1, April 2001) and were visually inspected for steric clashes with spacefilling models based on van der Waals radii. Superpositions where the ZBG occupied the same space as the protein were determined to be in steric conflict.

Results

Utilizing [(Tp^{Ph,Me})ZnOH] as a starting point,[5] we synthesized a number of complexes to serve as models of novel ZBGs bound to the active site of MMPs. Ternary complexes of [(Tp^{Ph,Me})ZnOH] have proven to be an accurate structural model for MMP active-site inhibition.[9,10] The series of ZBGs presented here can be separated into three groups: hydroxypyridinonate-based, *N*-methylated-hydroxypyridinonate-based, and hydroxypyridinonate derivatives. The complexes of [(Tp^{Ph,Me})Zn(ZBG)] have all been characterized by X-ray crystallography, ^{1}H/^{13}C NMR, IR, and elemental analysis.

The X-ray structures of hydroxypyridinonate-based ligands bound to the model complex show that these chelators coordinate in a bidentate fashion to the catalytic zinc(II) center (Figure 1). The ZBG 1-hydroxy-2(1*H*)-pyridinone is a cyclic analogue of hydroxamic acid and was therefore anticipated to bind in a chelating manner. In the structure of [(Tp^{Ph,Me})Zn(1-hydroxy-2(1*H*)-pyridinone)], the zinc center can be described as distorted trigonal bipyramidal (τ = 0.64)[21] with the 2-hydroxy oxygen atom and one of the pyrazole ring nitrogen atoms occupying the axial positions of the coordination sphere (Table 1). The coordinating oxygen atoms in this complex have Zn−O bond lengths of 1.97 Å (O1) and 2.09 Å (O2). These bond lengths are similar to the corresponding bond lengths in [(Tp^{Ph,Me})Zn(acetohydroxamate)], suggesting that this ZBG may bind with an affinity comparable to the hydroxamic acid ZBG.[10]

In the structure of [(Tp^{Ph,Me})Zn(3-hydroxy-2(1*H*)-pyridinone)], the zinc center can also be described as distorted trigonal bipyramidal (τ = 0.63, Figure 1) with one oxygen donor and one of the pyrazole rings occupying the axial positions of the coordination sphere (Table 1). This isomer

(18) Chen, L.; Rydel, T. J.; Gu, F.; Dunaway, C. M.; Pikul, S.; Dunham, K. M.; Barnett, B. L. *J. Mol. Biol.* **1999**, *293*, 545−557.
(19) Research Collaboratory for Structural Bioinformatics Protein Data Bank. http://www.rcsb.org/pdb/ (accessed July 2002).
(20) Puerta, D. T.; Schames, J. R.; Henchman, R. H.; McCammon, J. A.; Cohen, S. M. *Angew. Chem., Int. Ed.*, submitted for publication, **2003**.
(21) Addison, A. W.; Rao, T. N.; Reedijk, J.; van Rijn, J.; Verschoor, G. C. *J. Chem. Soc., Dalton Trans.* **1984**, 1349−1356.

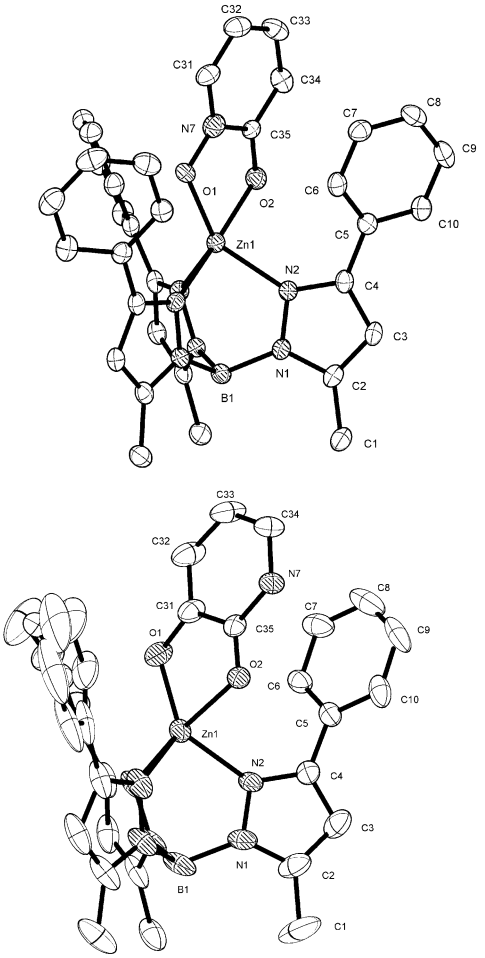

Figure 1. Structural diagrams of [(Tp^{Ph,Me})Zn(1-hydroxy-2(1*H*)-pyridinone)] (top) and [(Tp^{Ph,Me})Zn(3-hydroxy-2(1*H*)-pyridinone)] (bottom) with partial atom numbering schemes (ORTEP, 50% probability ellipsoids). Hydrogen atoms, solvent, and partial occupancy disorder (for [(Tp^{Ph,Me})-Zn(3-hydroxy-2(1*H*)-pyridinone)]) have been omitted for clarity.

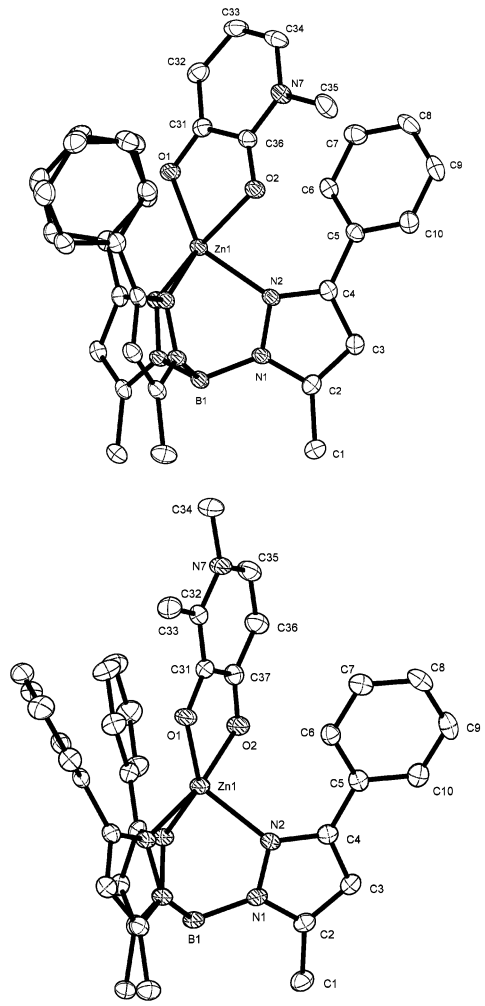

Figure 2. Structural diagrams of [(Tp^{Ph,Me})Zn(3-hydroxy-1-methyl-2(1*H*)-pyridinone)] (top) and [(Tp^{Ph,Me})Zn(3-hydroxy-1,2-dimethyl-4(1*H*)-pyridinone)] (bottom) with partial atom numbering schemes (ORTEP, 50% probability ellipsoids). Hydrogen atoms and solvent molecules have been omitted for clarity.

of 1-hydroxy-2(1*H*)-pyridinone has Zn−O bond lengths of 1.92 Å (O1) and 2.23 Å (O2), demonstrating strong bidentate coordination to the metal center.

The second group of ZBGs examined was the *N*-methylated-hydroxypyridinonate group. These ZBGs show similar binding to the unsubstituted hydroxypyridinonates (Figure 2). In the complex [(Tp^{Ph,Me})Zn(3-hydroxy-1-methyl-2(1*H*)-pyridinone)], the coordination environment around the zinc center can be described as distorted trigonal bipyramidal (τ = 0.52). The coordinating oxygen atoms are bonded to the model complex in a bidentate fashion with a Zn−O1 bond length of 1.94 Å and a Zn−O2 bond length of 2.21 Å (Table 3). The ZBG 3-hydroxy-1,2-dimethyl-4(1*H*)-pyridinone has the shortest averaged phenolic and carbonyl Zn−O bond lengths of all the novel ligands presented herein. The X-ray structure clearly demonstrates the tight binding of this ZBG with bond lengths of 1.96 Å (Zn−O1) and 2.05 Å (Zn−O2). The coordination environment is best described as distorted tetragonal (τ = 0.44) and is more distorted from trigonal bipyramidal than the other ZBGs described here.

The final group of novel ZBGs explored in this paper is classified as hydroxypyridinonate derivatives. This group includes 1-hydroxy-2(1*H*)-pyridinethione and 3-hydroxy-2-methyl-4-pyrone. The complex [(Tp^{Ph,Me})Zn(1-hydroxy-2(1*H*)-pyridinethione)] (Table 2) reveals that 1-hydroxy-2(1*H*)-pyridinethione binds in the expected bidentate fashion (Figure 3). The coordination environment around the zinc center can be described as distorted trigonal bipyramidal (τ = 0.54). The bond lengths of the coordinating sulfur and oxygen are longer than the coordinating oxygen atoms in the corresponding acetohydroxamic acid complex[10] because of the larger sulfur atom. In addition to the comparably longer Zn−S (2.32 Å) distance, the sulfur binding also affects the binding of the adjacent oxygen atom, increasing the Zn−O bond length to 2.08 Å (Table 3).

3-Hydroxy-2-methyl-4-pyrone binds to [(Tp^{Ph,Me})ZnOH], resulting in a complex (Figure 3) with comparable bond lengths as in [(Tp^{Ph,Me})Zn(acetohydroxamate)].[10] The Zn−O1 distance is 1.94 Å, and the Zn−O3 distance is 2.18 Å (Table 3). The coordination environment is similar to that of the hydroxypyridinonate ZBGs described above. The coordination sphere can be described as distorted trigonal bipyramidal (τ = 0.69) with one oxygen and one nitrogen donor occupying the axial positions.

Table 3. Bond Lengths for Coordinating Atoms in Complexes of [(Tp^{Ph,Me})Zn(ZBG)][a]

complex [(Tp^{Ph,Me})Zn(ZBG)]	Zn−O bond length for phenolic oxygen atoms (Å)	Zn−O bond length for carbonyl oxygen atoms (Å)
acetohydroxamic acid	1.976(1)	2.102(1)
1-hydroxy-2(1*H*)-pyridinone	1.967(2)	2.093(2)
3-hydroxy-2(1*H*)-pyridinone	1.918(2)	2.232(2)
3-hydroxy-1-methyl-2(1*H*)-pyridinone	1.935(1)	2.209(1)
3-hydroxy-1,2-dimethyl-4(1*H*)-pyridinone	1.965(1)	2.051(1)
1-hydroxy-2(1*H*)-pyridinethione	2.076(2)	2.325(1) (Zn−S)
3-hydroxy-2-methyl-4-pyrone	1.937(1)	2.185(1)

[a] All bond lengths were obtained from X-ray structure determinations.

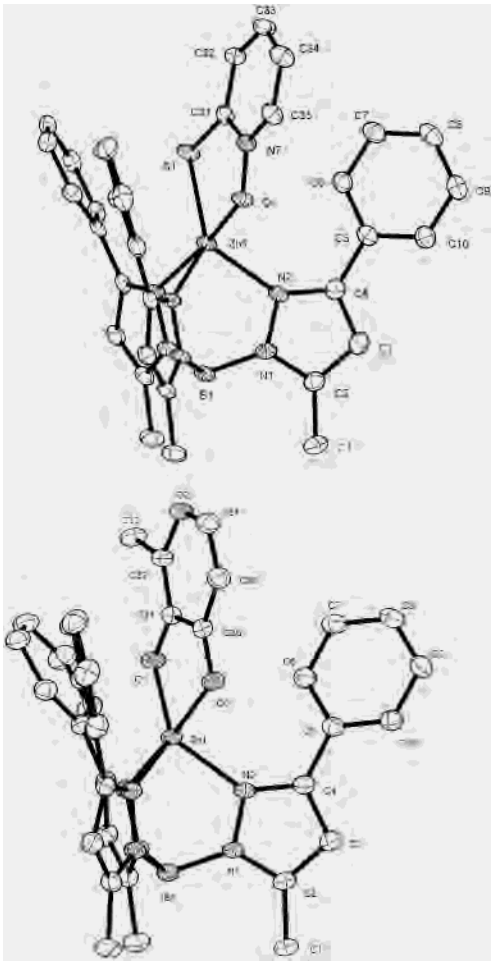

Figure 3. Structural diagrams of [(Tp^{Ph,Me})Zn(1-hydroxy-2(1*H*)-pyridinethione)] (top) and [(Tp^{Ph,Me})Zn(3-hydroxy-2-methyl-4-pyrone)] (bottom) with partial atom numbering schemes (ORTEP, 50% probability ellipsoids). Hydrogen atoms and solvent molecules have been omitted for clarity.

The solid-state structures of these ZBGs clearly demonstrate strong bidentate chelation of the zinc(II) metal centers. NMR spectra were acquired for all of the metal complexes to confirm ZBG coordination in solution. Large changes in the ^{1}H NMR spectra between the free and bound ZBGs support the stability of these complexes in solution. In the complex [(Tp^{Ph,Me})Zn(3-hydroxy-1-methyl-2(1*H*)-pyridinone)], significant shifts are observed in the ^{1}H NMR spectra. An unambiguous upfield shift is noticed for all protons in the ZBG bound to the metal center. These shifts are most likely the result of both the direct interaction of the chelator with the zinc(II) ion and the inclusion of the ZBG into the aromatic, hydrophobic pocket created by the Tp^{Ph,Me} ligand. For example, the proton para to the carbonyl group shifts from 6.24 ppm in the free ZBG to 6.01 ppm in the complex. In the complex [(Tp^{Ph,Me})Zn(3-hydroxy-2-methyl-4-pyrone)], the ^{1}H NMR also demonstrates from 0.5 to greater than 1.0 ppm changes in the proton resonances of the ZBG. Significant changes are also observed in the spectra of [(Tp^{Ph,Me})-Zn(1-hydroxy-2(1*H*)-pyridinethione)] relative to the free ZBG where again, in the ^{1}H NMR spectrum, notable shifts in the protons of the ZBG are observed. The ^{1}H NMR data suggest that the ligand binding observed in the solid state is preserved in solution at room temperature.

To further confirm the mode of binding, IR spectra were examined of the free ZBGs and compared to the corresponding zinc complexes. Cast films from $CHCl_3$ solutions onto NaCl plates of the ZBGs and complexes allowed for measurement of the carbonyl stretching frequencies. Appropriate B−H stretches were observed for the [(Tp^{Ph,Me})-Zn(ZBG)] complexes. All six of the ZBGs showed shifts in the C═O stretch to lower energy when complexed as [(Tp^{Ph,Me})Zn(ZBG)]. In the free ZBG 3-hydroxy-2-methyl-4-pyrone, the carbonyl (1624 cm^{-1}) exhibits a 27 cm^{-1} shift to lower wavenumbers in the metal complex (Figure S6). Similarly, comparison of the spectra of 1-hydroxy-2(1*H*)-pyridinone and of the complex [(Tp^{Ph,Me})Zn(1-hydroxy-2(1*H*)-pyridinone)] demonstrates a carbonyl shift from 1643 cm^{-1} for the free ZBG to 1625 cm^{-1} for [(Tp^{Ph,Me})Zn(1-hydroxy-2(1*H*)-pyridinone)]. The data here are consistent with other reports of changes in carbonyl stretching frequencies upon metal coordination.[22,23] All three ZBG classes (as defined above) demonstrate shifts in the carbonyl vibration consistent with the bidentate mode of binding found in the X-ray structures.

Computer modeling of these new ZBGs with human MMP-3 was performed to determine whether these chelators could fit within the MMP active site. The ZBG, zinc(II) ion, and coordinating nitrogen atoms from the model complexes were superimposed into a crystal structure of MMP-3.[18] The nitrogen atoms of the pyrazole model complexes do not uniquely correspond to any of the three histidine residues bound to the zinc(II) ion in the protein active site. Therefore, three orientations were scrutinized to reveal which superpositions allowed for the ZBG to reside in the active site without colliding with the protein surface. These studies generally yielded similar results regardless of the ZBG (Figures S1−

(22) Pecoraro, V. L.; Harris, W. R.; Wong, G. B.; Carrano, C. J.; Raymond, K. N. *J. Am. Chem. Soc.* **1983**, *105*, 4623−4633.
(23) Cohen, S. M.; Meyer, M.; Raymond, K. N. *J. Am. Chem. Soc.* **1998**, *120*, 6277−6286.

S5). Upon insertion to the protein crystal structure, the ZBGs either showed severe steric clashes with the protein, no steric clashes but with little or no room for attachment of a peptidomimetic "backbone" (required for MPI design),[1,24] or a binding conformation that showed no steric clashes and ample space for both the ZBG and a requisite drug "backbone". As a representative case, the three different conformations for the superposition of 3-hydroxy-2-methyl-4-pyrone are shown in Figure 4.

Discussion

Since MMPs were first linked to diseases such as arthritis and cancer, hydroxamate-derived drugs have been the staple for MPI design.[1] Hydroxamate-based inhibitors display good activity, and there are thousands of potential MMP inhibitors currently in some stage of the design process. We estimate that greater than 90% of these inhibitors utilize the hydroxamic acid-based ZBG.[1] There has been much effort placed to improve the design of better peptidomimetic "backbones" of MMP inhibitors, with the effort focused on enhancing the ZBG being relatively miniscule in comparison.

It has been shown that tris(pyrazolyl)borate complexes are good structural models for the active site of MMPs.[5−8] Using this model of the MMP active site, we synthesized a number of complexes to examine new routes to inhibitor design. All six complexes show that the novel ZBGs presented in this paper bind in a bidentate fashion. The bond lengths of the ZBGs to the zinc center are comparable to those in [($Tp^{Ph,Me}$)-Zn(acetohydroxamate)].[10] A better understanding of the interactions between the zinc(II) ion and the inhibitor is a recognized component of MPI design.[1,25,26] In this paper, we present six novel ZBGs that are proposed to further the understanding and scope of ZBGs for use in inhibitor design.

Using the successful hydroxamate ZBG as a starting point, we selected six new chelators that were expected to bind as well as or better than hydroxamates. Hydroxypyridinones (HOPOs) were selected as lead compounds for several reasons. HOPOs have a high structural homology to hydroxamic acids and are known to be strong metal chelators.[14,27−30] In addition, the cyclic structure of hydroxypyridinones reduces the degrees of freedom in the ligand, preventing the cis to trans isomerization that can occur in hydroxamic acids, which ultimately detracts from the thermodynamic affinity of the metal−ligand interaction. The basicity of hydroxypyridinones varies between isomers, which potentially allows for tuning the protonation state of the ligand to accommodate possible hydrogen-bonding interactions in the protein active

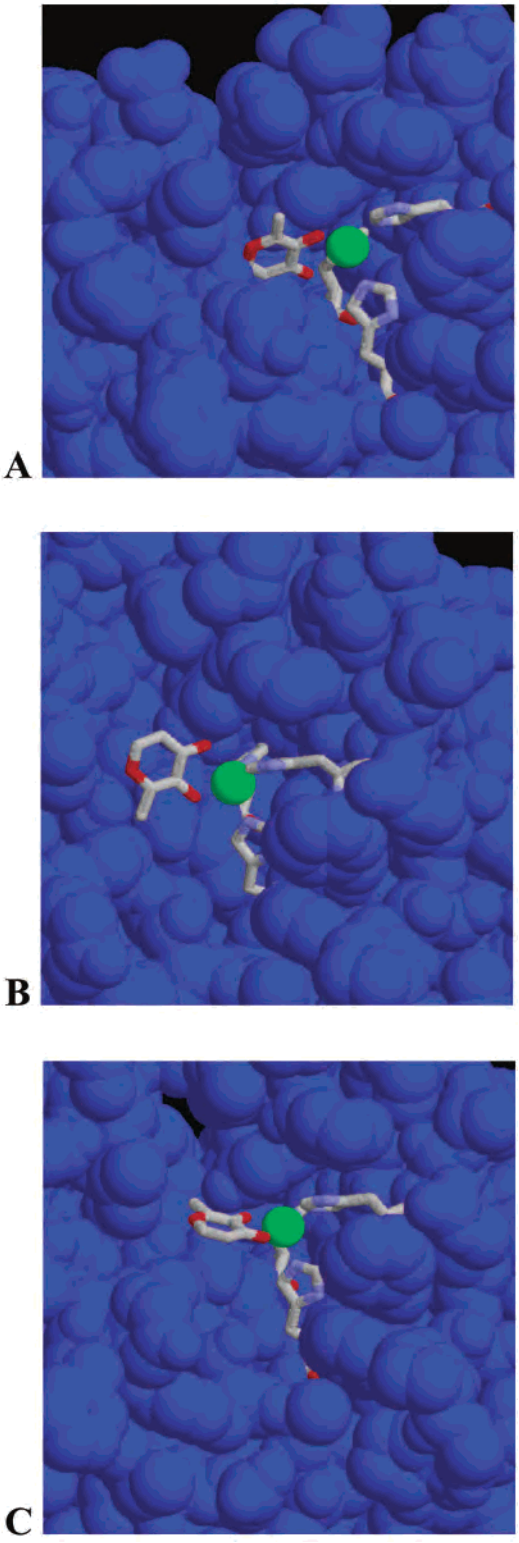

Figure 4. Images of model with insertion of 3-hydroxy-2-methyl-4-pyrone into the active site of MMP-3. Orientation A displays an obvious steric clash between the ring of the ZBG with the protein. Orientation B displays no steric clashes between the ZBG and protein; however, it also suggests that addition of a peptidomimetic "backbone" from the 2-methyl group would result in a steric clash. Orientation C demonstrates the least-steric obstacles for both the ZBG and a requisite drug "backbone." For clarity, the protein is shown in blue (space filling), zinc(II) in green (space filling), and His 201, 205, 211, and the ZBG are shown colored by element (stick models).

(24) Babine, R. E.; Bender, S. L. *Chem. Rev.* **1997**, *97*, 1359−1472.
(25) De, B.; Natchus, M. G.; Cheng, M.; Pikul, S.; Almstead, N. G.; Taiwo, Y. O.; Snider, C. E.; Chen, L.; Barnett, B.; Gu, F.; Dowty, M. *Ann. Proc. N.Y. Acad. Sci.* **1999**, *878*, 40−60.
(26) Matrisian, L. M. *Trends Genet.* **1990**, *6*, 121−125.
(27) Barnett, B. L.; Kretschmar, H. C.; Hartman, F. A. *Inorg. Chem.* **1977**, *16*, 1834−1838.
(28) Abu-Dari, K.; Karpishin, T. B.; Raymond, K. N. *Inorg. Chem.* **1993**, *32*, 3052−3055.
(29) Cohen, S. M.; Xu, J.; Radkov, E.; Raymond, K. N.; Botta, M.; Barge, A.; Aime, S. *Inorg. Chem.* **2000**, *39*, 5747−5756.
(30) Scarrow, R. C.; Riley, P. E.; Abu-Dari, K.; White, D. L.; Raymond, K. N. *Inorg. Chem.* **1985**, *24*, 954−967.

site.[24] Finally, many hydroxypyridinones and related compounds have been or are used in medical and food industry applications,[14,27,31] suggesting a reasonable level of biological tolerance for these chemical moieties.

Several hydroxypyridinone derivatives are also described, including *N*-methylated hydroxypyridinones, a hydroxypyridinethione, and 3-hydroxy-2-methyl-4-pyrone. These ligands share many of the same features as the hydroxypyridinones, but demonstrate other interesting features as well. The *N*-methylated hydroxypyridinones, 3-hydroxy-1-methyl-2(1*H*)-pyridinone, and 3-hydroxy-1,2-dimethyl-4(1*H*)-pyridinone were examined to show that substitutions on the hydroxypyridinone ring did not affect the binding or present steric problems toward zinc binding. This is important to demonstrate because these ZBGs will need to be appended with a peptidomimetic backbone to prepare a fully functional inhibitor. The hydroxypyridinethione, 1-hydroxy-2(1*H*)-pyridinethione, was examined to show that these sulfur derivatives also bind in a bidentate fashion to the zinc center. Sulfur-containing ligands of this sort may be very good ZBGs because of the apparent thiophilicity of zinc(II).[32,33] Similarly, other thiol-based MPIs have been studied[10] and have shown reasonably good activity when compared to hydroxamate-based inhibitors.[1,11,12] Combining the best features of both hydroxamates and thiol inhibitors into a single ZBG such as 1-hydroxy-2(1*H*)-pyridinethione should result in promising leads for future inhibitor design. Finally, 3-hydroxy-2-methyl-4-pyrone or "Maltol" (an FDA-approved food additive) was examined as a ZBG. Maltol also binds in a bidentate fashion with bond lengths similar to those of the other ZBGs. Maltol is an attractive ZBG because of its particularly good biological tolerance as evidenced by use as a food additive[34,35] and potential therapeutic applications as an insulin mimetic when complexed with vanadate.[31,36] These novel ZBGs demonstrate strong bidentate binding similar to that found in the complex [($Tp^{Ph,Me}$)Zn(acetohydroxamate)], which has been shown to be an accurate model for the MMP−inhibitor complex (Table 3).[10]

In addition to crystallographic, NMR, and IR data, computer modeling has been performed to explore the binding of the new ZBGs inside the active-site pocket of an MMP. This experiment was used to determine if any of the ZBGs would encounter steric problems upon binding. The structures of the complexes [($Tp^{Ph,Me}$)Zn(ZBG)] were fixed into the crystal structure of MMP-3,[18] with the histidine nitrogen atoms and the zinc(II) ion in the protein crystal structure aligned with the corresponding atoms from the model complex.[20] When placed in two of three possible orientations, the ZBGs were found to have no steric conflicts with the protein active site, and one of the three conformations appeared to be preferred for the development of inhibitors with a peptidomimetic substrate backbone (vide supra). These modeling studies are an essential first step toward performing computer-aided drug discovery using novel ZBGs.[20]

The design of potent and selective matrix metalloproteinase inhibitors presents the possibility to treat many diseases, including arthritis and cancer.[3] To date, no MPIs have completed phase III clinical trials.[4] A shift in the design process focused on higher affinity and more selective zinc-binding groups will aid in future drug development breakthroughs. We have successfully synthesized and characterized six [($Tp^{Ph,Me}$)Zn(ZBG)] complexes in an effort to demonstrate that new ZBGs are available for incorporation into MPIs. With binding comparable to that of the standard hydroxamate group, these alternative ZBGs give some fresh directions for the difficult endeavor of efficacious MPI design.

Acknowledgment. We thank an anonymous reviewer for identifying several important corrections to this manuscript; Dr. Peter Gantzel (U.C. San Diego), Prof. Arnold L. Rheingold (U.C. San Diego), and Dr. Charles Campana (Bruker AXS, Inc.) for help with the X-ray structure determinations; Julie R. Schames, Dr. Richard H. Henchman, and Prof. J. Andrew McCammon (U.C. San Diego) for assistance with the computer modeling; Dr. Jide Xu and Prof. Kenneth N. Raymond (U.C. Berkeley) for a gift of 3-hydroxy-1-methyl-2(1*H*)-pyridinone; Alexis Kaushansky for synthetic assistance; Prof. Emmanuel A. Theodorakis (U.C. San Diego) for use of his FT-IR; and Dr. Ulla Nørklit Andersen (U.C. Berkeley) for assistance with the elemental analysis. This work was supported by the University of California, San Diego, a Chris and Warren Hellman Faculty Scholar award (S.M.C.), a Hellman Fellowship (S.M.C.), and NIH Grant GM-60202-03 (D.T.P.).

Supporting Information Available: Figures S1, S2, S3, S4, S5, and S6. X-ray crystallographic files in CIF format. This material is available free of charge via the Internet at http://www.pubs.acs.org. X-ray crystallographic files in CIF format are also available via the Internet at http://www.ccdc.cam.ac.uk. Refer to CCDC reference numbers 192896, 192897, 192898, 192899, 192900, and 192901.

IC026029G

(31) Thompson, K. H.; McNeill, J. H.; Orvig, C. *Chem. Rev.* **1999**, *99*, 2561−2571.
(32) Sigel, H.; McCormick, D. B. *Acc. Chem. Res.* **1970**, *3*, 201−208.
(33) Lippard, S. J.; Berg, J. M. *Principles of Bioinorganic Chemistry*; University Science Books: Mill Valley, CA, 1994.
(34) Kim, M.-O.; Baltes, W. *J. Agric. Food Chem.* **1996**, *44*, 282−289.
(35) Wei, A.; Mura, K.; Shibamoto, T. *J. Agric. Food Chem.* **2001**, *49*, 4097−4101.
(36) Song, B.; Aebischer, N.; Orvig, C. *Inorg. Chem.* **2002**, *41*, 1357−1364.